Giant photon gain in large-scale quantum dot circuit-QED systems

Bijay Kumar Agarwalla,[1] Manas Kulkarni,[2] Shaul Mukamel,[3] and Dvira Segal[1]

[1]*Chemical Physics Theory Group, Department of Chemistry,*
and Centre for Quantum Information and Quantum Control,
University of Toronto, 80 Saint George St., Toronto, Ontario, Canada M5S 3H6
[2]*Department of Physics, New York City College of Technology,*
The City University of New York, Brooklyn, New York 11201, USA
[3]*Department of Chemistry, University of California, Irvine, California 92697, USA*
(Dated: June 1, 2021)

Motivated by recent experiments on the generation of coherent light in engineered hybrid quantum systems, we investigate gain in a microwave photonic cavity coupled to quantum dot structures, and develop concrete directions for achieving a giant amplification in photon transmission. We propose two architectures for scaling up the electronic gain medium: (i) N double quantum dot systems (N-DQD), (ii) M quantum dots arranged in series akin to a quantum cascade laser setup. In both setups, the fermionic reservoirs are voltage biased, and the quantum dots are coupled to a single-mode cavity. Optical amplification is explained based on a sum rule for the transmission function, and it is determined by an intricate competition between two different processes: charge density response in the gain medium, and cavity losses to input and output ports. The same design principle is also responsible for the corresponding giant amplification in other photonic observables, mean photon number and emission spectrum, thereby realizing a quantum device that behaves as a giant microwave amplifier.

Introduction.- Remarkable progress has been made in engineering, probing, and controlling hybrid light-matter systems which sit at the confluence of quantum optics and condensed matter physics [1–6]. Important examples include cavity-quantum electrodynamics arrays [7–9], trapped cold atoms coupled to photon degrees of freedom [10–13], interconnected copper waveguide cavities, each housing a qubit [14–16]. The successful integration of biased quantum dots (mesoscopic electronic systems) with a transmission line resonator (photonic degrees of freedom) has been a major step forward in this field [17–31]. Such quantum dot circuit-quantum-electrodynamics (QD-cQED) hybrids open up new directions for realzing quantum computing schemes based on localized electronic spins [32, 33], controlling electronic current via 'light' [34–37], and achieving high gain in the cavity transmission [1, 6]. Fundamentally, QD-cQED systems serve as a versatile platform for probing non-equilibrium open many-body quantum systems, by realizing basic models and phenomena in physics, for e.g., the Anderson-Holstein Hamiltonian with the fermionic system tuned to the Coulomb blockade or the Kondo regime [17, 28].

Focusing on the optical properties of the cavity, QD-cQED devices can be engineered and optimized to increase photon emission, by utilizing the voltage biased QDs as a gain medium [21, 24]. To significantly enhance optical signal in the cavity, recent efforts were focused on *scaling up* the gain-medium [38, 39]. A major advance in this regard has been the realization of a microwave laser (*maser*) via the fabrication of a *double* double quantum dot gain medium. In this setup, only when *both* electronic units were properly tuned to the cavity frequency did a maser action appear [40]. Despite impressive experimental demonstrations, a theoretical understanding of
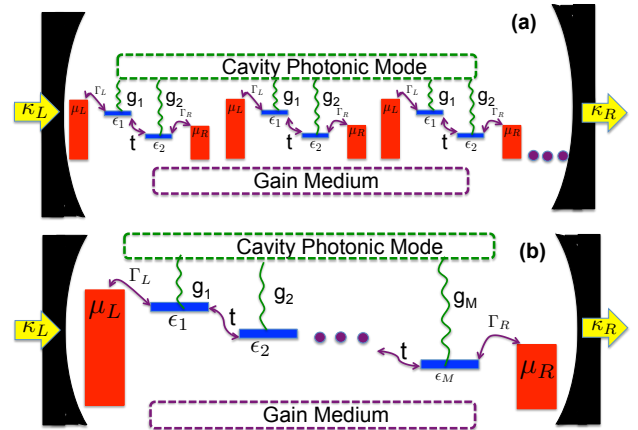

FIG. 1. (Color online) Schemes of large-scale quantum dot circuit-QED systems designed for achieving giant optical gain. A transmission line resonator is coupled via a Holstein-like interaction to an electronic gain medium with (a) N double quantum dots, each DQD tunnel-coupled to external electrodes and driven out-of-equilibrium by the application of a source-drain bias. (b) M dots in a cascade setup, with the first and last sites coupled to electronic leads. Tunnelling rates between the dots and the electron leads (Γ_L, Γ_R) and in between the dots (t) are tuned via gate-controlled tunnel-barriers. Cavity photons are coupled to the input and output ports with rates $\kappa_{L(R)}$. Arrows represent tunnelling processes and wavy lines indicate light-matter couplings.

principles governing amplification of photon emission in hybrid light-matter devices is missing. Specifically, what architectures, comprising large scale electronic quantum dot systems, can act as momentous gain media? How should we tune together the different couplings and driving forces to realize a giant microwave amplifier?

In this Letter, we describe from microscopic principles directions for enhancing photon emission, eventually reaching the lasing threshold—from below. We achieve a giant amplification of photonic observables (transmission, mean photon number, emission spectrum) by employing different large-scale gain media, (i) an N double quantum dot system (N-DQD) with each DQD maintained at a finite dc bias, see Fig 1(a), (ii) M dc-biased quantum dots arranged in series, see Fig 1(b). The second scenario is similar in spirit to the quantum cascade laser setup, and we refer to it as the Quantum Cascade (QC) model [41]. In both cases the electronic systems are coupled to the cavity with a *Holstein-like* light-matter interaction model. For the N-DQD system, a simple scaling law for the gain medium is identified, to reach giant amplification of photonic properties, significantly larger than a naive sum of individual gains for each DQD. In contrast, the QC device is missing such scalibility, yet we can identify cases beneficial for gain.

N-DQD Gain Medium.- We begin with the model displayed in Fig. 1(a) to explain the mechanism of photon amplification in the cavity. The electronic gain medium consists of N DQDs coupled to the same microwave cavity. Each DQD is further coupled to electronic leads at finite bias, denoted by $\Delta\mu = \mu_L - \mu_R$. The total Hamiltonian consists the N fermionic replicas, $\hat{H} = \sum_{i=1}^{N} \hat{H}_{el}^i + \sum_{i=1}^{N} \hat{H}_{el-ph}^i + \hat{H}_{ph}$, with $\hat{H}_{el}^i = \hat{H}_{QD}^i + \hat{H}_{lead}^i + \hat{H}_T^i$. Here $\hat{H}_{QD}^i = \epsilon\,(\hat{n}_{i1} - \hat{n}_{i2})/2 + t(\hat{d}_{i1}^\dagger \hat{d}_{i2} + h.c.)$ is the i-th DQD hamiltonian with ϵ as the detuning energy, t the hopping parameter, and $\hat{n}_{i1,i2} = \hat{d}_{i1,i2}^\dagger \hat{d}_{i1,i2}$ are the number operator for dots 1,2 respectively. Each DQD is connected to two electronic leads $\alpha = L, R$, $\hat{H}_{lead}^i = \sum_{k,\alpha} \epsilon_{k\alpha} \hat{c}_{ik\alpha}^\dagger \hat{c}_{ik\alpha}$, where k is the index for momentum, with the standard tunnelling Hamiltonian $\hat{H}_T^i = \sum_k v_{ikL} \hat{d}_{i1}^\dagger \hat{c}_{ikL} + \sum_k v_{ikR} \hat{d}_{i2}^\dagger \hat{c}_{ikR} + h.c.$ $\hat{d}$ and $\hat{c}$ are fermionic annihilation operators, $h.c$ denotes Hermitian conjugate. We define the spectral density for the electronic leads as $\Gamma_\alpha^i(\omega) = 2\pi \sum_k |v_{ik\alpha}|^2 \delta(\omega - \epsilon_{k\alpha})$. The photonic (bosonic) hamiltonian $\hat{H}_{ph}$ consists of the cavity mode of frequency ω_c, and two long transmission lines, left and right, $(K = L, R)$ with coupling ν_j to the cavity mode, $\hat{H}_{ph} = \omega_c \hat{a}^\dagger \hat{a} + \sum_{j\in K} \omega_{jK} \hat{a}_{jK}^\dagger \hat{a}_{jK} + \sum_{j\in K} \nu_j\,\hat{a}_{jK}^\dagger\,\hat{a} + h.c.$ The interaction between the microwave photon and the dipole moment of excess electrons in the DQDs is given by $\hat{H}_{el-ph}^i = g_i\,(\hat{n}_{i1} - \hat{n}_{i2})(\hat{a}^\dagger + \hat{a})$, with g_i as the coupling strength between the i-th DQD and the cavity. In what follows we assume that the DQDs replicas are identical, thus ignore the index i when appropriate.

We investigate the cavity response by focusing on the transmission function. Experimentally, such measurements are performed via heterodyne detection which can be realized here by interpreting the bosonic modes of the left and the right transmission lines as the input and output microwave signals, respectively. Following the input-output theory [42–44], the transmission function $t(\omega)$ (ratio of output vs input signal) for a single DQD ($N = 1$) can be expressed in terms of the response function of the cavity mode as

$$t(\omega) = \frac{i\kappa}{(\omega - \omega_c) + i\kappa - F_{el}^r(\omega)} = i\,\kappa\,D^r(\omega), \qquad (1)$$

where $D^r(t) = -i\,\theta(t)\,\langle[\hat{a}(t), \hat{a}^\dagger(0)]\rangle$ is the response function with the average performed over the combined electronic and photonic degrees of freedom. We further identify the electronic charge susceptibility in the time domain by $F_{el}^r(t - t') = g^2 \sum_{l,j=1,2}(2\,\delta_{lj} - 1)\Lambda_{lj}^{el}(t - t')$. Here

$$\Lambda_{lj}^{el}(t - t') = -i\,\theta(t - t')\,\left\langle\left[\hat{n}_l(t), \hat{n}_j(t')\right]\right\rangle_{el(g=0)} \qquad (2)$$

is the electron density response function, with the average performed over the electronic medium (dots and leads). In Eq. (1), $\kappa = \kappa_L = \kappa_R$ is the decay rate of the cavity mode per port [45]. Experimentally, it is large compared to $|F_{el}^r(\omega)|$ [21, 40].

Inspecting Eq. (1), we immediately identify a simple-fundamental principle for achieving gain, $|t(\omega)|^2 > 1$: We need to counteract the two different sources of response, the imaginary component of the gain medium-induced self-energy $F_{el}^{''}(\omega) \equiv \mathrm{Im}[F_{el}^r(\omega)]$, and the cavity decay rate to the ports. In other words, $F_{el}^{''}(\omega)$ should approach κ for achieving maximum gain. This objective cannot be accomplished at equilibrium, as $F_{el}^{''}(\omega) < 0$ [44]. Therefore, driving the electronic system out-of-equilibrium is a necessary condition for gain. Most significantly, from the causality condition of the retarded Green's function we receive the sum rule

$$\int_{-\infty}^{\infty} \frac{d\omega}{2\pi}\,t(\omega) = \frac{\kappa}{2}, \qquad (3)$$

valid for $\kappa > F_{el}^{''}(\omega)$. It tells us that an enhancement in maximum gain must be accompanied with the reduction in the width of the emission spectrum, thereby increasing the coherence time significantly, a critical requirement to eventually realize a maser [40]. Explicitly, $\int_{-\infty}^{\infty} \frac{d\omega}{2\pi}\,\mathrm{Re}[t(\omega)] = \kappa/2$ and $\int_{-\infty}^{\infty} \frac{d\omega}{2\pi}\,\mathrm{Im}[t(\omega)] = 0$.

Our objective is to enhance the electronic response $F_{el}^{''}(\omega)$ to reach high gain even for a poor (lossy) cavity with high rate κ. It can be optimized to a certain extent in a single DQD by tuning the metal-dot hybridization Γ and the bias voltage. We suggest an alternative, simple yet powerful, scalable approach: include N replicas of the DQD system to extensively-linearly increase the self-energy $F_{el}^r(\omega)$ [46]. For the case of N DQDs, the absolute value of the transmission, defined via $t(\omega) = |t(\omega)|e^{i\phi(\omega)}$, is now given as

$$|t(\omega)|^2 = \frac{\kappa^2}{\left[\omega - \omega_c - N\,F_{el}^{'}(\omega)\right]^2 + \left[\kappa - N\,F_{el}^{''}(\omega)\right]^2}, \qquad (4)$$
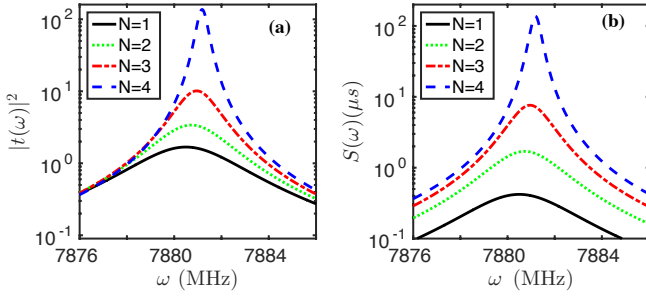
FIG. 2. (Color online) (a) Gain $|t(\omega)|^2$ and (b) emission spectrum $S(\omega)$ as a function of incoming frequencies ω for different number of DQDs. Parameters are $g = 50$ MHz, $\kappa = 3.15$ MHz, $\omega_c = 7880.5$ MHz, $\Gamma = 2.6$, $\epsilon = 7.0$, $t = 16.4$, $\Delta\mu = 250$, $k_B T = 0.69$, all in μeV.

with the area law $\int_{-\infty}^{\infty} \frac{d\omega}{2\pi} |t(\omega)|^2 = \frac{\kappa^2}{2\left[\kappa - N F_{el}''(\omega_c)\right]}$. Here, F_{el}' (F_{el}'') stands for real (imaginary) component of $F_{el}^r(\omega)$. It is clear that the transmission peak shifts from ω_c by $N F_{el}'(\omega_c)$, and the peak value is determined by the the difference between the electronic response and photon loss, $\kappa - N F_{el}''(\omega_c)$. Fig. 2 demonstrates this enhancement mechanism for a fixed detuning ϵ. With increasing number of DQDs, the transmission shows significant gain, as well as a reduction in width—close to the cavity frequency ω_c. In our parameters, $F_{el}''(\omega_c)$ approaches κ for $N_c = 4$, materializing giant gain. The detuning ϵ was chosen to satisfy a resonant condition, $\omega_c \sim \sqrt{\epsilon^2 + 4t^2}$. We later show that by searching for an optimal ϵ one can enhance the maximum gain by five orders of magnitude relative to the N=1 case.

Another relevant measure for the cavity response is the emission spectrum, induced by the electronic current, defined as $S(\omega) = \int_{-\infty}^{\infty} dt \langle \hat{a}^\dagger(0)\hat{a}(t)\rangle e^{i\omega t} = i D^<(\omega)$. It takes a structure similar to Eq. (4),

$$S(\omega) = i \frac{N F_{el}^<(\omega)}{\left[\omega - \omega_c - N F_{el}'(\omega)\right]^2 + \left[\kappa - N F_{el}''(\omega)\right]^2}, \quad (5)$$

and hence it can be similarly amplified, see Fig. 2(b). It immediately follows that $\int_{-\infty}^{\infty} \frac{d\omega}{2\pi} S(\omega) = \langle \hat{a}^\dagger \hat{a}\rangle \equiv \langle \hat{n}_c\rangle$.

Explicit expressions for the different components of the self energy, $F_{el}^{',''',<,>}(\omega)$, can be derived by employing a scheme based on the random-phase approximation, which is correct up to the second order of light-matter coupling but non-perturbative in the dot-lead coupling. With the help of Keldysh NEGF technique and the Langreth formulae [47], we receive the real and imaginary
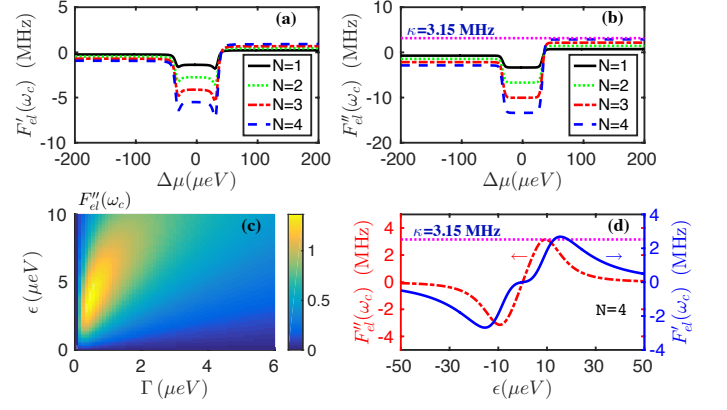

FIG. 3. (Color online) (a) Real ($F_{el}'(\omega_c)$) and (b) imaginary components ($F_{el}''(\omega_c)$) of $F_{el}^r(\omega)$ vs. bias difference $\Delta\mu$. (c) Two dimensional plot of $F_{el}''(\omega_c)$ as a function of dot-lead coupling Γ and detuning ϵ. (d) $F_{el}^{',''}(\omega_c)$ vs. ϵ for $N = 4$. Other parameters are same as in Fig. (2).
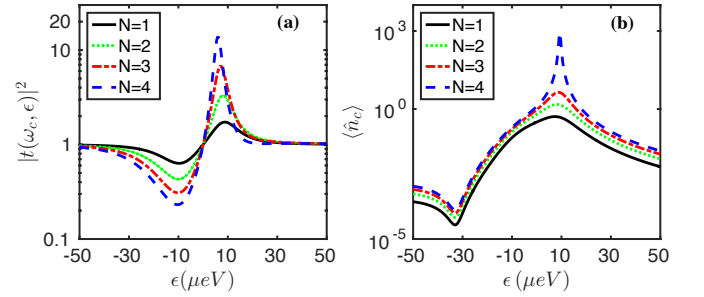

FIG. 4. (a) Gain $|t(\omega_c, \epsilon)|^2$ and (b) average photon number $\langle \hat{n}_c\rangle$ as a function of energy detuning ϵ for different number of DQDs. Other parameters are same as in Fig. 2.

components of the self energy as [48]

$$F_{el}'(\omega) = -i \int_{-\infty}^{\infty} \frac{d\omega'}{8\pi} \Big\{ \text{Tr}\Big[\mathbf{g}\, \mathbf{G}_0^k(\omega_+)\, \mathbf{g}\, \big(\mathbf{G}_0^r(\omega_-) + \mathbf{G}_0^a(\omega_-)\big)\Big]$$
$$+ \text{Tr}\Big[\mathbf{g}\, \mathbf{G}_0^k(\omega_-)\, \mathbf{g}\, \big(\mathbf{G}_0^r(\omega_+) + \mathbf{G}_0^a(\omega_+)\big)\Big]\Big\},$$
$$F_{el}''(\omega) = \int_{-\infty}^{\infty} \frac{d\omega'}{8\pi} \Big\{ \text{Tr}\Big[\mathbf{g}\, \mathbf{G}_0^k(\omega_+)\, \mathbf{g}\, \big(\mathbf{G}_0^r(\omega_-) - \mathbf{G}_0^a(\omega_-)\big)\Big]$$
$$- \text{Tr}\Big[\mathbf{g}\, \mathbf{G}_0^k(\omega_-)\, \mathbf{g}\, \big(\mathbf{G}_0^r(\omega_+) - \mathbf{G}_0^a(\omega_+)\big)\Big]\Big\}, \quad (6)$$

which depend on the reactive and dissipative parts of the electronic Green's functions respectively. Here, $\omega_\pm = \omega' \pm \frac{\omega}{2}$ and $\mathbf{g} = \text{diag}(g, -g)$. The nontrivial bias dependence enters through the Keldysh component $\mathbf{G}_0^k(\omega) = \mathbf{G}_0^<(\omega) + \mathbf{G}_0^>(\omega)$. Here $\mathbf{G}_0^{r,a}(\omega) = \big[\omega\mathbf{I} - \mathbf{H}_{QD} - \mathbf{\Sigma}^{r,a}(\omega)\big]^{-1}$ and $\mathbf{G}_0^{</>}(\omega) = \mathbf{G}_0^r(\omega)\mathbf{\Sigma}^{</>}(\omega)\mathbf{G}_0^a(\omega)$ follows the Keldysh equation. $\mathbf{\Sigma}^{r,a,</>}(\omega) = \mathbf{\Sigma}_L^{r,a,</>}(\omega) + \mathbf{\Sigma}_R^{r,a,</>}(\omega)$ are different components of the total self-energy, additive in the metallic leads, associated with the transfer of electrons between the metals and dots. $\mathbf{\Sigma}_L^{r,a}(\omega) = \text{diag}(\mp\frac{i\Gamma_L}{2}, 0)$, $\mathbf{\Sigma}_L^<(\omega) = \text{diag}\big(i f_L(\omega)\Gamma_L, 0\big)$,
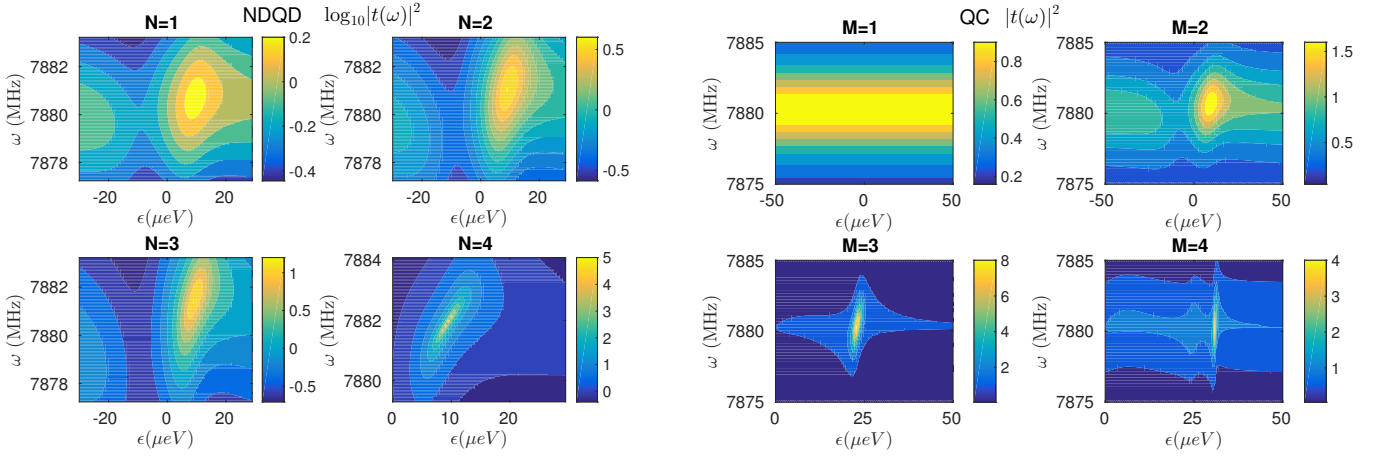
FIG. 5. Two dimensional plot of $|t(\omega)|^2$ as a function of ω and detuning ϵ for the N-DQD model (left 2×2 panels, also note the log_{10} scale) and the QC model (right 2×2 panels). Parameters are same as in Fig. 2.

$\boldsymbol{\Sigma}_L^>(\omega) = \text{diag}\left(-i[1-f_L(\omega)]\Gamma_L, 0\right)$. In writing the components $\boldsymbol{\Sigma}_L^{r,a}(\omega)$ we ignore the real part responsible for the renormalization of the DQDs' energies. Similar expressions hold for the right lead self-energy, with $\Gamma_L \to \Gamma_R$ and $f_L(\omega) \to f_R(\omega)$; $f_\alpha(\omega) = [e^{\beta(\omega-\mu_\alpha)}+1]^{-1}$ where β is the inverse temperature, identical for the photonic baths (ports) and the fermionic leads. For simplicity, in numerical calculations we assume the wide-band limit for the electronic leads, and take the metal-dots coupling to be symmetric ($\Gamma_L = \Gamma_R = \Gamma$). The lesser ($<$) and greater ($>$) components of $F_{el}(\omega)$ describe inelastic processes responsible for the exchange of energy between electrons and the cavity mode,

$$F_{el}^{</>}(\omega) = -i \int_{-\infty}^{\infty} \frac{d\omega'}{2\pi} \text{Tr}\left[\mathbf{g}\,\mathbf{G}_0^{</>}(\omega_+)\,\mathbf{g}\,\mathbf{G}_0^{>/<}(\omega_-)\right] \quad (7)$$

with $F_{el}^<(-\omega) = F_{el}^>(\omega)$, satisfying the detailed balance condition in equilibrium $F_{el}^>(\omega) = e^{\beta\omega}F_{el}^<(\omega)$.

We plot the real and imaginary components of $F_{el}^r(\omega_c)$ as a function of bias difference in Figs. 3(a,b). Close to equilibrium ($\Delta\mu < \omega_c$), both components are negative and the electronic system acts a dissipative bath. In contrast, far from equilibrium ($\Delta\mu > \omega_c$), $F_{el}''(\omega_c)$ saturates to a positive value, a necessary condition for observing gain. By further increasing the number of DQDs, $F_{el}''(\omega_c)$ approaches κ, to yield large gain (see Fig. 2). Note that even for a single DQD ($N=1$), a careful tuning of parameters allows for an enhancement of $F_{el}''(\omega)$, thus photon emission. This could be achieved by: (i) increasing the light-matter coupling strength g, as $F_{el}''(\omega)$ scales with g^2, (ii) tuning the dot-lead hybridization Γ. For weak Γ, the dwelling time of tunnelling electrons in the dots is long ($\sim 1/\Gamma$), resulting in an effectively-strong electron-photon interaction. (iii) As demonstrated in Figs. 3(c-d), by adjusting both level-detuning ϵ and Γ we can increase $F_{el}''(\omega_c)$ considerably. We exemplify the dependence of gain on detuning in Fig. 4(a). Both peak and dip in the

transmission, corresponding to photon emission and absorption events, respectively, are amplified upon increasing the number of replicas N. The corresponding plot for $F_{el}^{'/''}(\omega_c)$, for $N = 4$, is shown in Fig. 3(d).

The mean photon number in the cavity is another relevant observable $\langle \hat{n}_c \rangle = \langle \hat{a}^\dagger \hat{a} \rangle = i \int_{-\infty}^{\infty} \frac{d\omega}{2\pi} D^<(\omega)$. In the present low-temperature limit, $\beta\omega_c \gg 1$, it follows

$$\langle \hat{n}_c \rangle = \frac{i\,N\,F_{el}^<(\omega_c)}{2\left[\kappa - N\,F_{el}''(\omega_c)\right]}. \quad (8)$$

Therefore, it is again the competition between the charge density response and photon losses to the ports which determines the cavity photon number, see Fig. 4(b). For $N = 4$, giant photon number is observed, correlated with the associated high gain in the transmission function.

Quantum Cascade Model.- We next examine the cascade architecture, see Fig. 1(b). Here, multiple single-level quantum dots are sandwiched between source and drain leads. The transmission is determined by Eq. (1) with the electronic self-energy (6). In this case, $\mathbf{G_0}$ and $\boldsymbol{\Sigma}$ are $M \times M$ matrices made from the corresponding non-interacting dot Hamiltonian, and $\mathbf{g} = diag(g_1, g_2, \cdots, g_M)$. In simulations we used $g_1 = -g_2$, and $g_{j>2} = 0$, $\epsilon = \epsilon_{j+1} - \epsilon_j$, to allow a clear comparison with the N-DQD model [49]. It should be emphasized that in contrast to the N-DQD construction, the self-energy $F_{el}^r(\omega)$ for the cascade model shows a non-monotonic behavior with M.

Our results are summarized in Fig. 5, presenting significant photon amplification in the N-DQD and the QC models as a function of incoming photon ω and detuning ϵ, for different number of composite units. The N-DQD setup allows us to consistently enhance transmission with N, up to *five* orders of magnitude when $N = 4$. Note, we plot here $\log_{10}|t(\omega)|$. The QC model shows a moderate enhancement, as we explain next. For $M = 1$, the QC

model includes a single dot connected to metal leads, resulting in no optical gain $|t(\omega)|^2 \leq 1$, as the system lack a resonance condition. This can be proved by showing that $F_{el}^{''}(\omega)\big|_{M=1} < 0$ even far-from equilibrium [50] . We also observe in Fig. 5 that $M = 3$ operates better than $M = 2$, as in the former *two* resonant transitions contribute to photon emission around the cavity frequency. In contrast, $M = 4$ (and other even-valued QC setups) do not support degenerate transitions, thus transmission amplitude drops down to the $M = 2$ case. By carefully tuning the QC Hamiltonian one could engineer several resonant transitions, to receive significant amplification.

Conclusion.- We described a fundamental mechanism for optical amplification, by using large-scale hybrid quantum systems. Gain in the cavity transmission is explained via a sum rule for the transmission function, and it is achieved by counteracting the cavity decay rate to the ports with the gain-medium induced self-energy, the imaginary part of the charge density response function. This cancellation is in effect only far-from-equilibrium. We elaborated on this principle by testing two types of gain media: For an N-DQD setup, the extensive scaling of the electronic self-energy renders a direct route for realizing giant amplification in photon gain. For the quantum cascade model gain can be enhanced when the Hamiltonian supports degenerate transitions. Our theory approaches the lasing threshold $F_{el}^{''} = \kappa$ from below, as we are limited to the regime $F_{el}^{''} < \kappa$. Future work will involve investigations of the above-threshold regime, masing action and photon statistics.

[1] Z.-L. Xiang, S. Ashhab, J. Q. You, and F. Nori, Rev. Mod. Phys. **85**, 623 (2013).

[2] I. M. Georgescu, S. Ashhab, and F. Nori, Rev. Mod. Phys. **86**, 153 (2014).

[3] I. Buluta and F. Nori, Science **326**, 108 (2009).

[4] G Kurizkia, P. Bertetb, Y. Kubob, K. Molmerc, D. Petrosyand, P. Rablf, and J. Schmiedmayer, Proc. Natl. Acad. Sci. U.S.A. **112**, 3866 (2015).

[5] I.N. Hincks, C.E. Granade, T. W. Borneman, and D. G. Cory, Phys. Rev. Applied **4**, 024012 (2015).

[6] K. Le Hur, L. Henriet, A. Petrescu, K. Plekhnov, G. Roux, and M. Schiro, arXiv:1505.00167v2.

[7] A. A. Houck, H. E. Tureci, and J. Koch, Nat. Phys. **8**, 292 (2012).

[8] D. L. Underwood, W. E. Shanks, J. Koch, and A. A. Houck, Phys. Rev. A **86**, 023837 (2012).

[9] S. Schmidt and J. Koch, Annalen der Physik **525**, 395 (2013).

[10] K. Baumann, C. Guerlin, F. Brennecke and T. Esslinger, Nature **464**, 1301 (2010).

[11] M. Kulkarni, B. Öztop, and H. E. Türeci, Phys. Rev. Lett. **111**, 220408 (2013).

[12] S. Krinner, D. Stadler, D. Husmann, J.-P. Brantut, and T. Esslinger, Nature **517**, 64 (2015).

[13] R. Mottl, F. Brennecke, K. Baumann, R. Landig, T. Donner, and T. Esslinger, Science **336**, 1570 (2012).

[14] C. Aron, M. Kulkarni, and H. E. Türeci, Phys. Rev. X, **6** 011032 (2016).

[15] M. E. Schwartz, L. Martin, E. Flurin, C. Aron, M. Kulkarni, H. E. Tureci, and I. Siddiqi, arXiv:1511.00702.

[16] C. Aron, M. Kulkarni, and H. E. Türeci, Phys. Rev. A **90**, 062305 (2014).

[17] M. R. Delbecq, V. Schmitt, F. D. Parmentier, N. Roch, J. J. Viennot, G. Fve, B. Huard, C. Mora, A. Cottet, and T. Kontos, Phys. Rev. Lett. **107**, 256804 (2011).

[18] M. R. Delbecq, L. E. Bruhat, J. J. Viennot, S. Datta, A. Cottet, and T. Kontos, Nat. comm. **4**, 1400 (2013).

[19] J. J. Viennot, M. R. Delbecq, M. C. Dartiailh, A. Cottet, and T. Kontos, Phys. Rev. B **89**, 165404 (2014).

[20] K. D. Petersson, L. W. McFaul, M. D. Schroer, M. Jung, J. M. Taylor, A. A. Houck, and J. R. Petta, Nature **490**, 380 (2012).

[21] Y.-Y. Liu, K. D. Petersson, J. Stehlik, J. M. Taylor, and J. R. Petta, Phys. Rev. Lett. **113**, 036801 (2014).

[22] S. Ashhab, J.R. Johansson, A.M. Zagoskin, and F. Nori, New J. Phys. **11**, 023030 (2009).

[23] T. Frey, P. J. Leek, M. Beck, A. Blais, T. Ihn, K. Ensslin, and A. Wallraff, Phys. Rev. Lett. **108**, 046807 (2012).

[24] A. Stockklauser, V. F. Maisi, J. Basset, K. Cujia, C. Reichl, W. Wegscheider, T. Ihn, A. Wallraff, and K. Ensslin, Phys. Rev. Lett. **115**, 046802 (2015).

[25] H. Toida, T. Nakajima, and S. Komiyama, Phys. Rev. Lett. **110**, 066802 (2013).

[26] M. Kulkarni, O. Cotlet, and H. E. Türeci, Phys. Rev. B **90**, 125402 (2014).

[27] G.-W. Deng, D. Wei, J. R. Johansson, M.-L. Zhang, S.-X. Li, H.-O. Li, G. Cao, M. Xiao, T. Tu, G.-C. Guo, H.-W. Jiang, F. Nori, and G.-P. Guo, Phys. Rev. Lett. **115**, 126804 (2015).

[28] L. E. Bruhat, J. J. Viennot, M.C. Dartiailh, M. M. Desjardins, T. Kontos, and A. Cottet, Phys. Rev. X **6**, 021014 (2016).

[29] G.-W. Deng, L. Henriet, D. Wei, S.-X. Li, H.-O. Li, G. Cao, M. Xiao, G.-C. Guo, M. Schiro, K. Le Hur, and G.-P. Guo, arXiv:1509.06141.

[30] C. Xu and M. G. Vavilov, Phys. Rev. B **88**, 195307 (2013).

[31] J. Jin, M. Marthaler, P.Q. Jin, D. Golubev, G. Schön, New J. Phys **15**, 025044 (2013).

[32] J. J. Viennot, M. C. Dartiailh, A. Cottet, and T. Kontos,

Science **349**, 408 (2015).

[33] N. Lambert, F. Nori, and C. Flindt, Phys. Rev. Lett **115**, 216803 (2015).

[34] C. Bergenfeldt and P. Samuelsson Phys. Rev. B **85**, 045446 (2012).

[35] C. Bergenfeldt and P. Samuelsson Phys. Rev. B **87**, 195427 (2013).

[36] L. D. Contreras-Pulido, C. Emary, T. Brandes, and R. Aguado, New J. Phys. **15**, 095008 (2013).

[37] N. Lambert, C. Flindt, and F. Nori, Europhys. Lett. **103**, 17005 (2013).

[38] A. Cottet, C. Mora, and T. Kontos, Phys. Rev. B **83**, 121311 (2011).

[39] C. Karlewski, A. Heimes, and G. Schön, Phys. Rev. B **93** 045314 (2016).

[40] Y.-Y. Liu, J. Stehlik, C. Eichler, M. J. Gullans, J. M. Taylor, and J. R. Petta, Science **347**, 285 (2015).

[41] J. Faist, F. Capasso, D. L. Sivco, C. Sirtori, A. L. Hutchinson, A. Y. Cho, Science **264**, 5158 (1994).

[42] A. A. Clerk, M. H. Devoret, S. M. Girvin, F. Marquardt, and R. J. Schoelkopf, Rev. Mod. Phys. **82**, 1155 (2010).

[43] M. Schiro and K. Le Hur, Phys. Rev. B **89**, 195127 (2014).

[44] O. Dmytruk, M. Trif, C. Mora, and P. Simon, Phys. Rev. B **93**, 075425 (2016).

[45] In the wide-band limit we define $\kappa = 2\pi\rho|\nu|^2$, where ρ is the photon bath density of states and ν being the average coupling between the cavity and the bath modes.

[46] The linear scaling of F_{el}^r with the number of electronic units in the N-DQD model is valid in the present weak coupling limit, $g/\omega_c \ll 1$, as different dissipation/response terms affect the cavity mode in an additive manner.

[47] J. Rammer, *Quantum Field Theory of Non-Equilibrium States*, Cambridge University Press, (2007).

[48] B. K. Agarwalla, M. Kulkarni, S. Mukamel, and D. Segal, arXiv:1604.01811.

[49] Though only the first two dots are coupled to the cavity mode, in the eigenenergy representation of the cascade all transitions are coupled to the microwave mode.

[50] It can be shown that in the $M=1$ cascade model with $\Gamma_L = \Gamma_R = \Gamma$,

$$F_{el}^{''}(\omega)\big|_{M=1} = g^2 \int_{-\infty}^{\infty} \frac{d\omega'}{4\pi} f_n(\omega') A(\omega') \big[A(\omega'-\omega) - A(\omega'+\omega) \big]$$

with $f_n(\omega) = [f_L(\omega) + f_R(\omega)]/2$ as the non-equilibrium distribution function and $A(\omega) = i[G_0^r(\omega) - G_0^a(\omega)]$ the spectral function for a single-dot model. The integral of the first term is always smaller than the second term.